Bull. Chem. Soc. Jpn., ***68***, *771—774(1995)*

A Voltage-Modified Trajectory Simulation for a State-Selected CH_3I Supersonic Beam in an Electrostatic Hexapole Field

Dock-Chil Che, Tetsuya Ogawa,# Hiroshi Ohoyama, Toshio Kasai,* and Keiji Kuwata

Department of Chemistry, Faculty of Science, Osaka University, Toyonaka, Osaka 560

(Received September 13, 1994)

The $|JKM>$ state selection of a seeded CH_3I/Ar supersonic beam has been achieved using a 2-m electrostatic hexapole field. Several $|JKM>$ states were better resolved than the previous one in a CH_3Cl/He supersonic beam. A voltage-modified trajectory simulation was carried out for fitting the observed focusing curve, in which the first-order approximation of the Stark effect was corrected in terms of the hexapole voltage in an empirical formula. A better agreement was found on the peak positions of the focusing curve, and the relative heights of the three peaks suggest that CH_3I molecules in the present beam populate among the $|JKM>$ states in a statistical way with a rotational temperature of 3 K.

Molecules in a supersonic molecular beam can be focused and state-selected in a single $|JKM>$ rotational state using an electrostatic hexapole field,[1—4] where J, K, and M are the total angular momentum of a symmetric top molecule, its projection on the molecular axis and the electric field direction, respectively.[5] The assignment of the peaks of a focusing curve (the beam intensity transmitted through the hexapole field vs. the hexapole rod voltage) has been achieved mostly by computer simulations. Gandhi and co-workers have performed the single rotational state-selection of a Kr seeded CH_3I molecular beam; they assigned the resolved states by simulations.[1] Although the simulations have shown the good agreement with the experiment on the whole, the agreement regarding the peak positions assigned to $|313>$, $|211>/|312>$ at higher voltages appear to be unsatisfactory.[1] Stolte and co-workers have studied CH_3F and N_2O molecular beams using a wobbling electrostatic hexapole field, where the signal difference between the in-axis and the off-axis was measured.[2,3] A simulation of the focusing curve has shown good agreement, except for a disagreement at the highest voltages, again. Kasai and co-workers have measured the focusing curve of CH_3Cl using a 2-m hexapole field; the conventional Monte Carlo trajectory simulation, however, was not able to fit the $|211>/|312>$ peak at higher voltages.[4]

There seems to be a trend that a simulated focusing curve shows unsatisfactory agreements in the peak position at higher voltages of the hexapole field.[1—4,6] In general, higher order Stark effects become effective at higher voltages; neglecting those effects may cause a peak shift along the axis of V_0.[6] Thus, the disagreement in the peak position of the focusing curve could be solved by taking into account higher order Stark effects. The peak height of a focusing curve reflects the populations of the corresponding $|JKM>$ rotational states of molecules in a beam; they are regarded as being statistical in most cases. However, since this assumption is not necessarily obvious for molecules in a supersonic beam, the reliability of this assertion needs to be confirmed by computer simulations. Second, the peak width of a focusing curve is formed due to several factors regarding the initial velocity distribution and the angular divergence of the beam. The peak width is also affected by the alignment conditions of the beam assembly. In the present study, we measured the focusing curve of CH_3I using a 2-m electrostatic hexapole field for separating single $|JKM>$ states. By developing a voltage-modified Monte Carlo trajectory simulation, the focusing curve was analyzed in order to clarify how the experimental factors influence the shape of the focusing curve.[7] A comparison of the results is made between the conventional and modified-trajectory methods.

Experimental and Trajectory Simulations

1. Single $|JKM>$ State Selection. A supersonic beam of 2% CH_3I seeded in Ar was produced with a 0.8 mmϕ pulsed value at 200-Torr stagnation pressure (1 Torr= 133.322 Pa), and skimmed by a 1.0 mmϕ skimmer. Unfocused molecules in the beam, such as CH_3I with $K=0$ and CH_3I/Ar clusters with no permanent dipole moment, were removed by a 1.1 mmϕ beam-stop set in front of the hexapole field, where the $|JKM>$ state-selection was performed. The

---

#Present address: Department of Electronic Engineering, Faculty of Engineering, Osaka University, Yamadaoka, Suita, Osaka 560.

beam intensity, detected as CH$_3$I$^+$, was measured as a function of the hexapole rod voltage (V_0) by a quadrupole mass spectrometer through a 1 mmϕ inlet aperture. A detailed description of the apparatus for selecting single $|JKM>$ rotational states was given in a previous paper.[4)]

2. Conventional and Voltage-Modified Monte Carlo Trajectory Simulation. In first-order perturbation theory the perturbed energy (ΔW_1) of CH$_3$I in an electric field is given by[8—12)]

$$\Delta W_1 = \boldsymbol{\mu}\cdot\boldsymbol{E} = \mu E < \cos\theta >= \mu EKM/J(J+1), \quad (1)$$

where μ is the permanent electric dipole moment of CH$_3$I, E is the strength of the electric field applied to the molecule, and θ is the angle between the molecular axis and the electric field direction. Molecules in a $|JKM>$ rotational state are state-selected and focused in a hexapole field at a specific hexapole rod voltage (V_{JKM}) if the sign of the KM product is negative,

$$V_{JKM} = \pi^2 v^2 R^3 mJ(J+1)/(6\mu L^2 KM), \quad (2)$$

where m is the mass of CH$_3$I, v is the velocity, R is the inner radius of the hexapole field, and L is the electric field length, which is set to be equal to the focal length.[8)] In the conventional simulation, the first-order approximation of Stark effect is assumed. This approximation should be adequate at low voltages.[5)] However, higher order Stark effects should become important at high voltages and when molecules pass very near to the hexapole rods, since the amplitude of the n-th term is proportional to the n-th power of the electric field strength (E). Their contribution increases rapidly with an increment of E. For instance, the second-order stark effect is given by Eq. 3,[5)]

$$\Delta W_2 = (\mu^2/2Bh)[f(J,K,M) - f(J+1,K,M)]\,|\,E\,|^2, \quad (3)$$

where $f(J,K,M)=(J^2-K^2)(J^2-M^2)/[J^3(2J-1)(2J+1)]$ and B is the rotational constant of the molecule. Equation 3 tells us that the sign and strength of the second-order Stark energy (ΔW_2) depend upon values of J, K, and M of the $|JKM>$ state.

Figure 1 shows the calculated ratios ($\Delta W_2/\Delta W_1$) of the energy for the second-order Stark effect to the first-order one when $V_0=5.5$ kV is applied; they are calculated as a function of the radial distance (r) in the hexapole field. As mentioned, the sign and strength of the energy for the second-order Stark effect depend upon the $|JKM>$ state. For instance, the upper curve of the figure is for $|211>$ and the lower one for $|312>$, and their V_0-dependence is different. ΔW_2 of the $|211>$ state is positive and that of the $|312>$ state is negative, while ΔW_1 is always positive for both states. In addition, the former state gives a larger ratio than the latter. The electric field strength increases in proportion to the square of r, and the neighborhood of the electrodes at 7 mm gives the highest contribution from the second-order Stark effect in the present case, where ΔW_2 of $|211>$ becomes 7% of the first-order Stark energy, and ΔW_2 of $|312>$ becomes 2%. Thus, the contribution of the second-order Stark effect can be regarded as being substantial in the vicinity of the electrodes. Besides the field strength, the number of trajectories increases according to the weight of $2\pi r dr$ as the radial distance increases. As far as the sign of ΔW_2 is concerned, these two $|JKM>$ states may behave in an opposite way. It would be complex, however, to estimate how the trajectories of molecules are perturbed by higher order Stark effects. The force exerted on a molecule in the field should be determined point by point from the gradient of the local potential in the field. It is difficult to estimate how trajectories are affected without performing exact numerical simulations, though such simulations would be too complex to carry out in practice.

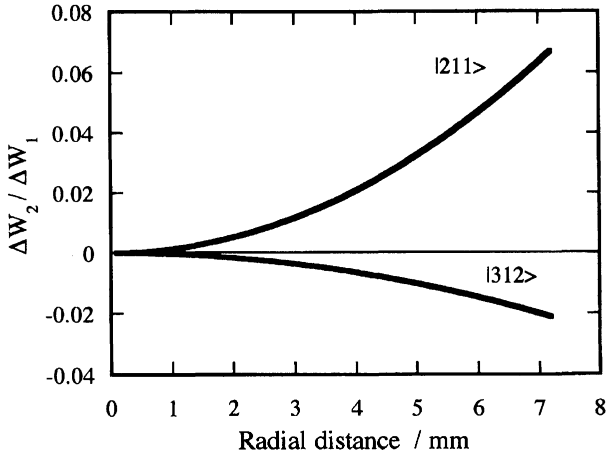

Fig. 1. Simulated ratios of energy of the second-order Stark effect ΔW_2 to the first-order one ΔW_1 for $|211>$ (the upper curve) and $|312>$ (the lower curve). The ratios are calculated as a function of the radial distance in the hexapole field at $V_0=5.5$ kV.

It is therefore desirable to modify the conventional trajectory simulation, in which contributions from higher order effects are considered. We present a simple method which includes higher order Stark effects as a correction term to the hexapole rod voltage (V_0). Namely, the conventional simulation is modified by introducing an effective voltage (V_{eff}) in place of V_0. V_{eff} is an effective rod voltage to molecules in the hexapole field, and molecules are assumed to move under a first-order perturbation. In turn, V_{eff} should be exactly equal to V_0 in the conventional simulation. As the hexapole rod voltage is increased, molecules would begin to experience an interaction under V_{eff} which is larger than the nominal V_0. Let us assume that V_{eff} may be expressed by a power series of V_0 as the following formula shows:

$$V_{\text{eff}} = V_0 + \alpha V_0^2 + \beta V_0^3 + \cdots, \quad (4)$$

where α and β are expansion coefficients for the second-order and the third-order terms, and other higher order terms follow. Though this is an expansion of V_{eff}, the terms higher than the first order would represent the corresponding contribution from higher order Stark effects through the V_0 change within the first-order Stark effect.

Besides the higher order Stark effects, there should also be additional factors that might affect the trajectories and that might produce some deviation in the simulation. The use of a cylindrical approximation for the hexapole electrodes,[13)] and the use of an effective length of the field are such factors, but cannot be easily determined theoretically and are normally assumed to be adjustable parameters in the conventional simulation. Equation 4 might be a sort of expression for making corrections for such factors in a trajectory simulation.

Each simulated point was obtained by calculating 2×10^5 trial trajectories which satisfy the initial conditions of the molecular beam prepared in the experiment: the initial distributions of the rotational states, the velocity, and the angular divergence. They were reproduced by a Monte Carlo method.[7] Trajectories with no collisions at the beam-stop, the collimator walls and the hexapole rods were counted as a successful trajectory. The rotational state distribution for J and K was assumed to be statistical in the beginning. The J levels were truncated at $J=70$ for computational convenience in reproducing a Boltzmann distribution.

Results and Discussion

Figure 2 shows the focusing curve of a 2% CH_3I/Ar supersonic beam. The data points are indicated by open circles. The experimental error at each point remains within the circle size. The rod voltage (V_0) was scanned from 0 to 7.0 kV in steps of 0.05 kV. The peaks of the focusing curve are nicely resolved. The separation of neighboring peaks was found to be better than in the previous result for a CH_3Cl/He supersonic beam.[4] This is, perhaps, because of the different seeding conditions. The focusing curve obtained by the conventional trajectory simulation under the first-order Stark effect is indicated by the solid line in the figure. As mentioned in the previous section, the relative peak heights determine the rotational populations of CH_3I, so that they are directly related to the rotational temperature (T_r) in a Boltzmann distribution. A good agreement was obtained when T_r was chosen to be 3 K, indicating that the CH_3I molecules populate among the $|JKM>$ states statistically. (Note that the $|JKM>$ states up to $J=70$ are all included in the simulation). We discuss this point in more detail later. As for the peak position along the V_0 axis, however, an unsatisfactory agreement is seen between the calculated curve and the experimental one. This disagreement becomes serious near to the third peak at higher voltages. In order to clarify the cause, any effects of an imperfect alignment of the beam assembly were first tested in a trajectory simulation. This could occur if the mass spectrometer is not set exactly on the right position in the beam centerline.

Figure 3 shows the results of a simulation when the mass spectrometer was set out of the beam centerline on purpose. As can be seen in the figure, an imperfect alignment of the detector produces little change in the peak position of the focusing curve if it is as small as 0.5 mm. However, as the imperfect alignment becomes larger, the peak shift begins to occur to a significant extent. It was found that all peaks of the curve move toward higher V_0 simultaneously as the imperfect alignment exceeds 1.0 mm. The tendency of this simultaneous peak shift indicates that an imperfect alignment of the detector is not the main cause of the observed disagreement, because the large shift appears only at the higher region of V_0, as shown in Fig. 2.

Figure 4 shows the best-fit result of a voltage-modified trajectory simulation. After many trials, the simulations within the second-order term were found to give unsatisfactory agreement. We thus employed modifications up to the third term. The best-fit was obtained with coefficients of $\alpha=-0.017$ and $\beta=-0.0012$, respectively. It was found that β should be much smaller than α by an order of magnitude, but should not be zero. As can be seen in Fig. 4, the calculated peak positions are in good accord with the experiment. The first two peaks at hexapole voltages of 2.1 and 3.3 kV are assigned to the $|111>$ and $|212>$ states, respectively. The third peak at 5.5 kV is assigned to the $|211>/|312>$ state, since $|JKM>=|211>$ and $|312>$ give the same value of the average orientation, i.e. $<\cos\theta>=KM/(J^2+J)=$

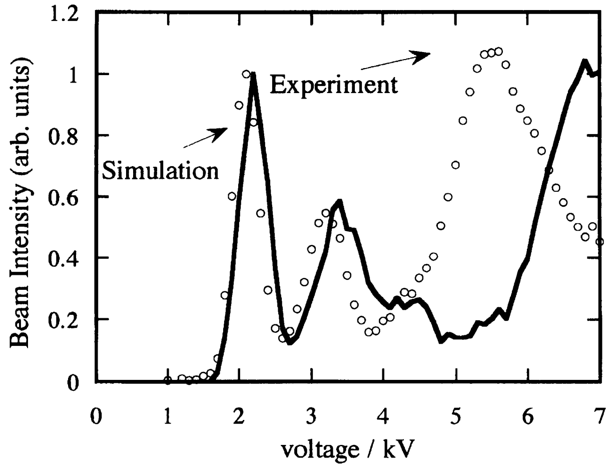

Fig. 2. Focusing curve of the 2% CH_3I/Ar supersonic beam. Beam intensity was measured on the CH_3I^+ parent mass peak. Experimental errors are within the circles. The solid curve was obtained by the conventional trajectory simulation with a rotational temperature of 3 K.

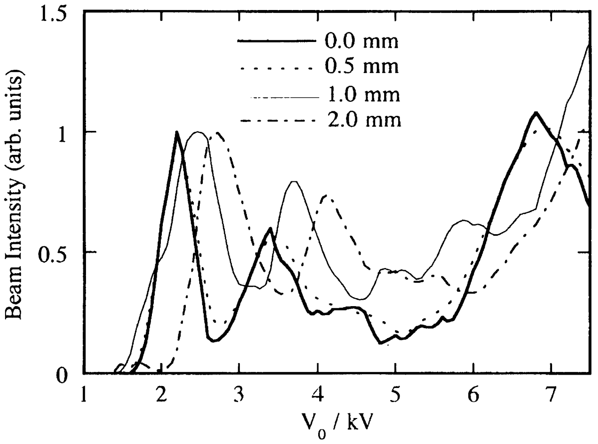

Fig. 3. Effect of an imperfect alignment of the beam assembly. The solid line shows a perfect alignment (the deviation of the mass spectrometer is zero); the dashed line, the thin solid line, and the broken line show imperfect alignments with 0.5, 1.0, and 2.0 mm deviation, respectively.

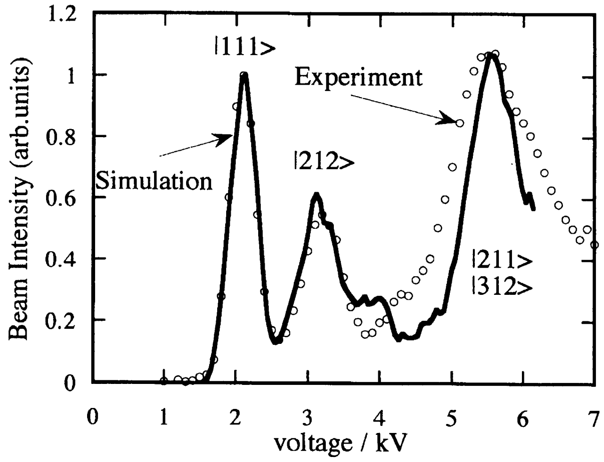

Fig. 4. Voltage-modified trajectory simulation for the focusing curve of the 2% CH_3I/Ar supersonic beam. The peak assignment was done as $|JKM>=|111>$, $|212>$, and $|211>/|312>$ from left to right by the simulation.

1/6. A common feature of the focusing curve is that we only observe the states $K=1$, because the rotational temperature is very low in a supersonic beam and the K levels have a larger rotational constant than that of the J levels in the case of pencil-type symmetric top molecules, like CH_3I. On the whole, the peak positions and the peak heights of the curve show excellent agreement with the experimental result after using a voltage-modified simulation. However, we must admit that the simulated peak of the $|211>/|312>$ state seems to be narrower than the observed one. A part of the reason for this may be that the higher order Stark effect for $|211>$, and $|312>$ must affect in the opposite direction of V_0, as shown in Fig. 1. Thus, practical trajectories can be blurred and the peak width broadened. On the other hand, the voltage-modified trajectory simulation does not take this situation into account. Second, the use of an effective rod voltage in the first Stark approximation might compress the peak width, especially at high voltages. Nonetheless, the present simulation method is regarded as being useful for assigning the focusing curves; otherwise, the conventional simulations always failed.

The best-fit rotational temperature was obtained when $T_r=3$ K. The ratio of the populations of the first two peaks, $|111>$ and $|212>$, is $1:0.62$. The simulations show that it changes to $1:0.48$ at 2 K, and $1:0.70$ at 4 K. Thus, the rotational temperature could be determined rather accurately in the present simulation. Though the J levels are truncated at $J=70$ in generating the rotational state distribution, the Boltzmann distribution appears to reproduce the observed population properly. In principle, it could be possible to assume a non-Boltzmann distribution for the $|JKM>$ states, since arbitrary combinations of J, K, and M produce a peak at the desired V_0 using the relation $<\cos\theta>=KM/(J^2+J)$. However, a preliminary calculation with such a non-statistical distribution tells us that unrealistic population, like $|111>:|212>:|414>=1:0.54:1.05$ have to be assumed in order to fit the observed curve, and that the population cannot be determined uniquely. We thus tentatively conclude that the rotational distribution of CH_3I in the present supersonic beam is statistical. It was found that the 2-m hexapole field is adequate to separate the single $|JKM>$ states of CH_3I, and that the voltage-modified trajectory simulation can be applied for the assignment of the resolved peaks of the focusing curve. For rationalizing the present simulation method, a theoretical confirmation may be necessary in future studies.

The present work was partially supported by a Grant-in-Aid for Scientific Research No. 05640571 from the Ministry of Education, Science and Culture.

References

1) S. R. Gandhi, T. J. Curtiss, Q.-X. Xu, S. E. Choi, and R. B. Bernstein, *Chem. Pyhs. Lett.*, **132**, 6 (1986).

2) H. Jalink, D. H. Parker, K. H. Meiwes-Broer, and S. Stolte, *Chem. Phys.*, **108**, 391 (1986).

3) M. H. M. Janssen, D. H. Parker, and S. Stolte, *J. Phys. Chem.*, **95**, 8142 (1991).

4) T. Kasai, T. Fukawa, T. Matsunami, D.-C. Che, K. Ohashi, Y. Fukunishi, H. Ohoyama, and K. Kuwata, *Rev. Sci. Instrum.*, **64**, 1150 (1993).

5) C. H. Townes and A. L. Shawlow, "Microwave Spectroscopy," Dover, New York (1955), Chap. 10.

6) F. Harren, D. H. Parker, and S. Stolte, *Comments At. Mol. Phys.*, **26**, 109 (1991).

7) T. Kasai, K. Ohashi, H. Ohoyama, and K. Kuwata, *Chem. Phys. Lett.*, **127**, 581 (1986).

8) K. H. Kramer and R. B. Bernstein, *J. Chem. Phys.*, **42**, 767 (1965).

9) P. R. Brooks and E. M. Jones, *J. Chem. Phys.*, **45**, 3449 (1966).

10) R. J. Beuhler, Jr., R. B. Bernstein, and K. H. Kramer, *J. Am. Chem. Soc.*, **88**, 5331 (1966).

11) S. E. Choi and R. B. Bernstein, *J. Chem. Phys.*, **85**, 4463 (1985).

12) J. Reuss, "Atomic and Molecular Beam Methods," ed by G. Scoles, Oxford University, London (1988), Chap. 11.

13) J. J. Everdij, A. Huijiser, and N. F. Verster, *Rev. Sci. Instrum.*, **44**, 721 (1973).